# International Journal of Engineering Research and Science & Technology

IJERST

ISSN : 2319-5991

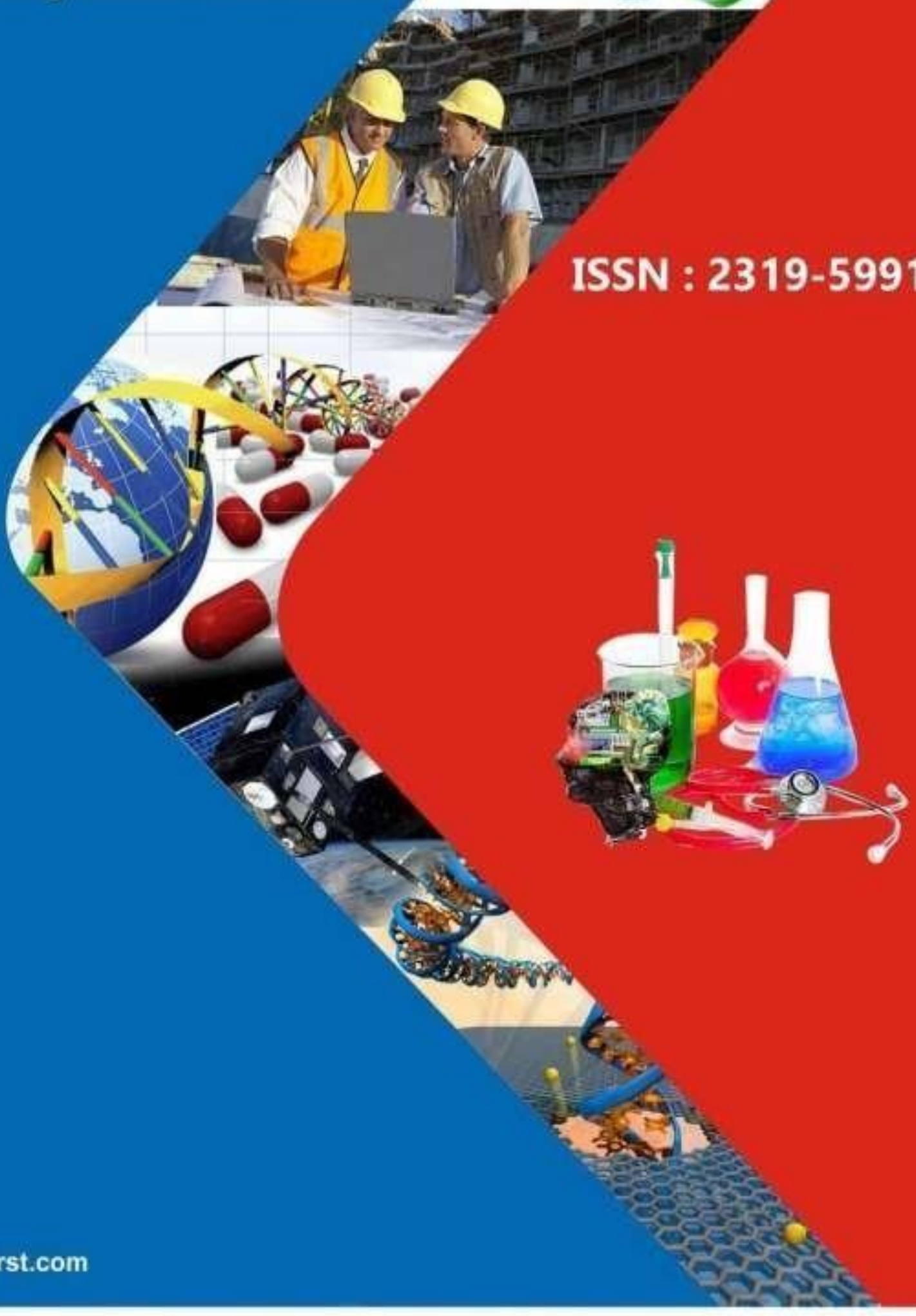

www.ijerst.com

Email: editor@ijerst.com or editor.ijerst@gmail.com

International Journal of Engineering Research and Science & Technology

ISSN 2319-5991 www.ijerst.com

Vol. 17, Issue.2, 2024

# REACTIVE POWER SYNCHRONIZATION METHOD FOR CONTROLLING GRID-FORMING CONVERTERS IN RENEWABLE ENERGY PLANTS

*[1]MR. S.Bala Naik, [2]Narayandas Karthik, [3]M. Lokesh, [4]V. Luhith kumar*

*[1](Assistant professor), EEE.Guru Nanak Institutions Technical Campus, Hyderabad.*

*[234]B.Tech Scholars, EEE. Guru Nanak Institutions Technical Campus, Hyderabad*

## ABSTRACT

In recent years, synchronous generators (SGs) from traditional power plants have been displaced by the tremendous influx of renewable energy sources into electrical networks. Because of the way they operate, electronic power converters, which are often used to link renewable energy facilities to power grids, are unable to provide the same power generating services as SGs. In an effort to mimic the performance of SGs, many ideas for electronic converter control have been put forward recently, leading to the creation of what are known as grid-forming converters (GFCs). In order to separate the synchronizing power and the active power management of a renewable generating source that has a converter linked, this study suggests a novel GFC control technique based on the reactive power synchronization (RPS) method. Three power sources are evaluated in this research for this purpose: photovoltaic (PV) plants, batteries, and full-converter wind turbines. Additionally, the research suggests models and controls for every one of these sources, whose dynamics have a significant impact on the grid services that renewable energy facilities provide. Subsequently, the research suggests a GFC–RPS control system and validates its efficacy in various scenarios. One such scenario is inertial response, which promptly supplies power via a rapid frequency response following a load fluctuation on a grid. PV plants, in contrast to wind turbines and storage systems, can only provide these services when they are not using their full power. The research also confirms the efficacy of the GFC–RPS control approach for controlling AC voltage at a converter's output terminals. Lastly, when feeding a dynamic load, the article evaluates GFC hot swapping during the switch from a grid-connected to an isolated operating mode. Findings showed that the voltage and frequency stay constant, proving that the suggested GFC-RPS control does, in fact, function as a real voltage source and mimic the characteristics of a traditional SG.

Index Terms: Grid-forming power converter, quick frequency response, hot switching of converters, renewable energy sources, and reactive power synchronization.

## 1.INTRODUCTION

In the context of microgrids, the idea of grid-forming converters (GFCs) was first presented [1], [2] as a novel control technique for voltage source converters (VSCs), which function as uninterruptible power supplies and are intended to maintain voltage and frequency at the load in the event that it disconnects from microgrids. Since GFCs have low series resistance and function as voltage sources, synchronization mechanisms need to be precise enough to enable concurrent operations with other GFCs providing isolated loads.

However, because of the extensive integration of renewable energy sources into power networks in recent years, the development of GFC has taken on a higher significance. Synchronous generators (SGs) used in traditional power plants are gradually being replaced with electronic power converters, which are often used to link renewable energy sources to the grid. Traditionally, these SGs have managed the electrical networks' voltage and frequency. Many European electricity systems' current energy generation scenarios show that, during specific times, a very high percentage of energy demand (>70%) is met by renewable generation; some nations are even suggesting that, in the upcoming decades, renewable energy will meet 100% of the total energy demand [3].From a grid perspective, SGs function as voltage sources, while converters in gridfollowing mode are seen as voltage-controlled current sources. The following grid services are outlined in international grid regulations [4] as operational requirements for renewable generation: a) power/frequency management; b) reactive/voltage control; and c) supply continuity in the case of voltage dips (e.g., fault ride through). The issue with grid-following converters is that, while they are referred to be grid supporting, they always supply their services after voltage and frequency are sensed at their terminals. For instance, a phase-locked loop (PLL) is used to monitor frequency variations in order to raise or reduce active power while performing a power–frequency (P/f) control service. This technique simulates how SG governors work. However, when simulating the inertial response of these generators at very high electronic converter penetration rates, several studies indicate that they might cause grid instability [4], [5]. An imbalance between the active power produced and consumed in an electrical system leads to frequency variation. Because grid-following converters use frequency to detect imbalances and adjust their behavior appropriately, they always provide services after a power imbalance impact has occurred. Converters operating in this mode in a synchronous generating situation will initially maintain frequency, but they won't be able to manage it entirely on their own. As a result, renewable energy sources are often prohibited from providing local loads that are disconnected from the grid and are required to include "anti-islanding" safeguards [6]. Moreover, GFCs often mimic SG behavior. In these cases, the integral action of the frequency deviation, 1ω, which is calculated through an active power synchronization loop, or through reactive power as the current study suggests, replaces the orientation angle (θ) of the control system, which was previously determined by measuring voltage directly at converter terminals through a PLL. A number of studies on GFC grid synchronization techniques have been published recently, while the most of them have concentrated on active power synchronization loops [7]–[11]. The design of active power synchronization techniques against phase jump, frequency deviation, imbalance, disturbance rejection, and voltage harmonics is covered in references [7]–[9]. Moreover, the stability of synchronization procedures in weak grids and during voltage dips is investigated in [10], [11]. The most basic synchronization technique uses a droop regulator to calculate frequency increase, 1ω, depending on the departure of active power from a predetermined reference value [12]–[14]. Zhang et al. presented the first synchronization strategy for VSC converters linked to a grid without a specialized synchronization unit in [15], despite the fact that this technology has been extensively employed in microgrid applications.

Although this synchronization technique was first suggested for use with high-voltage direct current (HVDC) converters, it has since been expanded to include additional uses. This method mimics the synchronizing torque that SGs naturally provide by using controls. This prompted some researchers to suggest simulating an SG's oscillation equation using controlled-operated power synchronization loops. A virtual synchronous machine (VSM) is the name given to these controllers [14], [16], and [17]. Similar methods are the foundation of a synchronverter [18], which simulates SGs without the need of a synchronization unit. Lastly, [19] introduces a synchronous power converter (SPC), the working concept of which is based on the application of a second-order function to the variation between the measured and reference active powers in order to determine frequency deviation, or 1ω. When there is a discrepancy between the reference frequency and the frequency recorded by a PLL, this method employs an extra frequency loop to adjust the active power reference. A comparable method based on reactive power synchronization (RPS) also exists [20]–[24]. All of the aforementioned strategies use an active power synchronization (APS) loop. Based on the dynamic equations of the interconnectivity grid, this method is based on the relationship between the active and reactive powers that are rapidly transferred by the GFC. The frequency control technique known as GFC-RPS was first put forward in [20] for the internal grid of offshore wind farms that were coupled to HVDC cables via LCC rectifiers. Offshore wind farms may employ uncontrolled rectifiers (including units using diode rectifiers) since their electricity flows in a single direction. In comparison to HVDC-VSC rectifiers, these rectifiers are more durable and more reasonably priced, but in order to switch, they need a steady AC grid.

This paper suggests a central approach that uses a capacitor bank to sustain a GFC that is coupled to the input terminals at a rectifier station. Subsequently, [22] spoke about how controls may be implemented without capacitors. The authors used a distributed version of the same control approach in [21]. Here, the front-end

International Journal of Engineering Research and Science & Technology

ISSN 2319-5991 www.ijerst.com

Vol. 17, Issue.2, 2024

converters of full-converter (FC) wind turbines distribute reactive power produced by a wind turbine farm fairly while also maintaining the frequency of the internal AC grid. The authors of [23] evaluated the control techniques used to synchronize converters to a grid by monitoring reactive power, as well as the dynamic connection between active and reactive powers. This idea has the benefit that the dynamics of the renewable energy source won't effect the synchronization loop, leaving the active power channel open. Furthermore, [24] suggests expanding on the RPS idea and using it to regulate FC wind turbines' dispersed frequencies in black-start scenarios. Hot swapping—the process of switching between isolated and grid-connected modes of operation, or vice versa—is another crucial component of GFC functioning. Nonetheless, this shift suggests a significant disruption in voltage and frequency [50]–[52]. The majority of control strategies covered in earlier research use the assumption that there is a perfect DC voltage source in the DC connection that can provide all of the energy required by the AC terminals. Nonetheless, the dynamics of the source really affect GFC reactions in wind turbines and solar facilities. In particular, GFC control mechanisms using RPS applied to renewable generating sources (batteries, solar plants, and wind generators) are covered in this work. Additionally, it evaluates and analyzes how they react to changes in frequency, AC voltage regulation, and when switching between connected to the grid and isolated modes of operation. The structure of this document is as follows: A system overview is given in Section II, and fundamental RPS concepts are covered in Section III with regard to a basic grid made up of a GFC coupled to a voltage source with an impedance of Zg and represented by its dynamic equations. In addition, Section III derives transfer functions for increases in active and reactive power in terms of voltage and angle module modifications and suggests a linear model in the state space. The RPS control system, a block diagram for the plant model, and RPS controls are then presented in Section IV. In a similar manner to an SG, the resultant oscillation equation is computed as a second-order function that creates a link between fluctuations in active power and angle. In Section V, active power regulation methods and models of renewable energy plants for sources linked to a converter are covered. In addition, Section VI looks into regulator designs, and Section VII presents the outcomes of the simulations run for every technology under consideration. In particular, Section VII discusses how GFC reacts to changes in grid load, how AC voltage is controlled, how to switch between grid-connected and isolated modes, and how to feed a dynamic load into converter terminals in the event that a circuit breaker trips. Finally, our study's results are covered in Section VIII.

## 2.POWER QUALITY

Like many other business sectors, the container crane industry of today is often mesmerized by the bells and whistles, vibrant diagnostic displays, high speed performance, and degrees of automation that may be attained. We must remember the foundation upon which we are constructing even if these capabilities and their indirectly linked computer-based innovations are essential to an effective terminal operation. The glue that holds the Foundation blocks together is called power quality. The dependability of cranes, our environment, terminal operational economics, and the initial investment in power distribution infrastructure to support new crane installations are all impacted by power quality. "Using electricity wisely is a good environmental and business practice which saves you money, reduces emissions from generating plants, and conserves our natural resources," said the utility company newsletter that was sent with my most recent monthly bill. Performance standards for container cranes are, as everyone knows, rising at an incredible pace. Future container cranes will need an average power need of 1500–2000 kW, which is about twice as much as the entire average demand from three years ago. These cranes are now in the bidding process. In the near future, there will be a greater awareness of the power quality problem due to the sharp rise in power demand levels, the population growth of container cranes, the retrofitting of SCR converter crane drives, and the size of the AC and DC drives required to power and operate these cranes.

PROBLEMS WITH POWER QUALITY

Power quality issues are defined as "any power problem that results in failure or misoperation of customer equipment, manifests itself as an economic burden to the user, or produces negative impacts on the environment" for the purposes of this article.

Regarding the container crane sector, the following power-related problems deteriorate power quality:

• Harmonic distortion; power factor; voltage transients; voltage swells and sags;

## 3. PROPOSED SGCC CONTROLLER

The block diagram of the 4Q GCC controller and its schematic are shown in Fig. 3.1 in a rotating reference frame. These kinds of configurations are often seen in distributed energy generating systems, such as wind and solar power plants [9]–[10]. This paper discusses a controller architecture that requires a quicker HIL with a 1μs PWM sampling time since it uses a 4kHz PWM carrier frequency. PWM sampling frequency should, as a general rule, be at least 256 times greater than the carrier frequency. Furthermore, an HIL system has to have an intuitive and user-friendly tool chain (Fig. 3), which enables the designer to rapidly describe the hardware of the power electronics system, assign analog and digital inputs and outputs, control contactors, alter the waveforms of the grid voltage, and more.

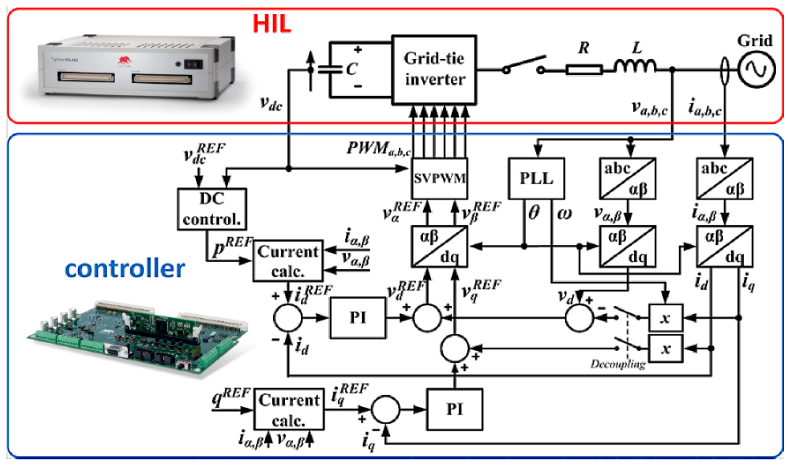


Fig. 3.1. The schematic of the grid tie inverter (upper frame) modelled in the HIL device, and the controller (lower frame) under test.

Fig. 3.1 displays the schematic and block diagram of the 4Q GCC controller in a rotating reference frame. Distributed energy producing systems, including wind and solar power plants, often use these sorts of arrangements [9]–[10]. This study presents a controller design that employs a 4kHz PWM carrier frequency, which necessitates a faster HIL with a 1μs PWM sampling time. Generally speaking, the PWM sampling frequency need to be at least 256 times higher than the carrier frequency. An HIL system must also include an easy-to-use and intuitive tool chain (Fig. 3), which allows the designer to quickly define the power electronics system's hardware, assign analog and digital inputs and outputs, regulate contactors, modify the grid voltage waveforms, and more.

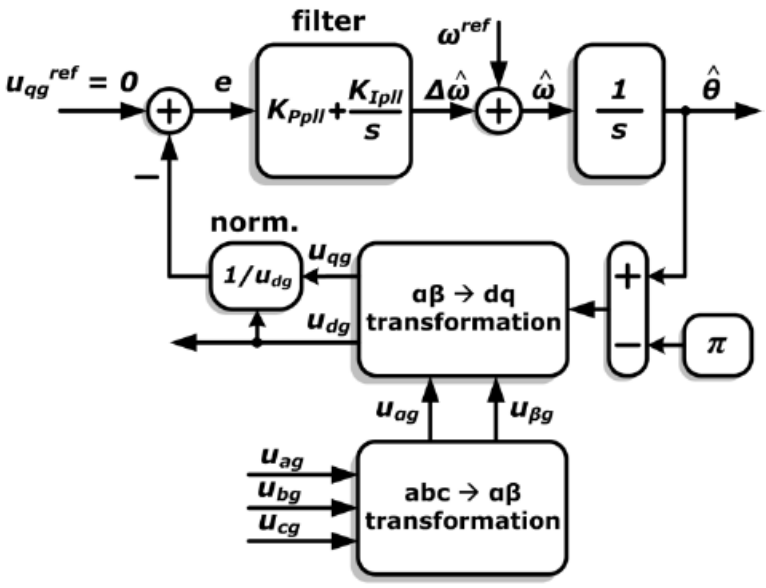


Fig. 3.2. dq-PLL system block diagram

PLL functionality must be carefully designed to strike the best balance between disturbance rejection and the response speed required to accurately track grid voltage during frequency changes or voltage distortions like voltage sags, as these factors have a significant impact on the functionality of the grid and grid measurement imperfections such as unbalanced voltage, harmonic distortion, and measurement offsets [12]. It is shown that the following values must be entered for the critical-aperiodic PLL response filter parameters (KPpll and KIpll):

International Journal of Engineering Research and Science & Technology

ISSN 2319-5991 www.ijerst.com

Vol. 17, Issue.2, 2024

$$K_{P_{pll}} = \sqrt{2}\omega_{bw} \quad K_{I_{pll}} = \frac{\omega_{bw}^2}{2} \qquad (1)$$

where ωbw is the necessary PLL system bandwidth [12]. For the required frequency bandwidth of 3 Hz, the expected PLL angle response settling time would be around one second. The HIL environment might be used for this evaluation. under particular, significant HIL test automation of real controller hardware and software may be completed under a number of scenarios, including interruptions. It is clear that offline simulations are insufficient for testing and verifying real controller designs. In this test, grid voltage waveforms with 3.5% of the fifth and seventh harmonics are used. To mimic measurement errors, a 5% offset is introduced to the "grid" voltage and the phase b and phase c amplitudes are reduced to 90% and 95%, respectively (Fig. 6).

## 4.PHASE LOCKED LOOP

A control system that seeks to produce an output signal whose phase is connected to the phase of the input "reference" signal is known as a phase-locked loop, or phase lock loop (PLL). This electrical circuit compares the phase of the signal obtained from the oscillator to an input signal using a variable frequency oscillator and a phase detector. In a feedback loop, the oscillator is controlled by the phase detector signal. The circuit adjusts the oscillator's frequency to maintain phase matching by comparing the phases of the input and output signals that are generated from it.

Phase is the derivative of frequency. Maintaining lock step in both the input and output phases also means maintaining lock step in the input and output frequencies. Thus, an input frequency may be tracked by a phase-locked loop, or it can produce a frequency that is a multiple of the input frequency. Indirect frequency synthesis uses the latter attribute, whereas demodulation uses the former.

In radio, telephony, computers, and other electrical applications, phase-locked loops are commonly utilized. They may distribute clock timing pulses in digital logic devices like microprocessors, recover a signal from a noisy communication link, or provide steady frequencies. With output frequencies ranging from a fraction of a hertz to several gigahertz, the approach is frequently utilized in current electronic systems because one integrated circuit may supply a whole phase-locked-loop building block.

Useful parallels

An analogy from motor racing:

Take a look at a car race to get a realistic understanding of what's happening. Every one of the several automobiles is trying to complete the course as quickly as possible. Every lap represents a whole cycle, and a vehicle may perform several dozen laps in an hour. While the number of laps (a distance) relates to a phase, the number of laps per hour (a speed) is a frequency. Car 3 may have completed 37.23 laps at one point in time.

Every vehicle is competing against every other car on the track for the majority of the race. On the other hand, a pace vehicle arrives to establish a safe speed in the event of a collision. Each racing vehicle wants to remain as close to the pace car as possible, but none of them are allowed to overtake it or the race cars in front of it. The pace car serves as a reference while it is on the course, and the racing vehicles turn into phase-locked loops. Every driver will calculate the phase difference—a measurement expressed in laps—between himself and the lead vehicle. In order to close the distance if the driver is too far away, he will accelerate his engine (the VCO). He will slow down if he gets too near to the pace vehicle. As a consequence, every racing vehicle locks onto the pace car's phase. In a fraction of a lap, the vehicles go in close formation around the circuit.

An analogy with a clock

A phase difference may be a time difference since phase and time can be proportionate. Clocks are phase-locked, or time-locked, to a master clock to varied degrees of precision.

Every clock will tell the time at a slightly different pace if left on its own. For example, a wall clock may differ from the NIST reference clock by a few seconds every hour. That time differential would grow over time to be significant.

Every week, the owner resets his wall clock and does a phase comparison to ensure that it is in sync with the time on his wall clock. If nothing changes, the wall clock will still deviate from the reference clock by a few seconds per hour.

A fast-slow control, or time adjustment, is included in some clocks. The owner discovered his wall clock was running too quickly when he compared its time to the reference time. As a result, he could slightly alter the timing to slow down the clock's operation. If all goes according to plan, his clock will be more precise. The wall clock's perception of a second would coincide with the reference time over a sequence of weekly adjustments (within the wall clock's stability).

1921 saw the introduction of the Shortt-Synchronome clock, which used an early mechanical form of a phase-locked loop.

## 5 PROPOSED SYSTEM MODELLING

A grid-forming regulated voltage source electronic converter coupled to a grid is the system layout shown in Fig. 5.1. The input current is Idc, while the voltage across the DC bus terminals is Vdc. An LC filter is used to link the converter to the point of common coupling (PCC). Measurements of the grid current (ig), PCC voltage (V), and current (i) are used to manage the GFC. The instantaneous values of reactive power (Qg) and active power (Pg) are computed at the grid connection point of the GFC. The GFC's operating mode is then determined by the status of a breaker that is attached between the PCC terminals and the grid (on: grid connected, off: islanded). A voltage source with an amplitude of Vg, frequency of ωg, short-circuit impedance of Zg, and ratio of X/R forms the Thévenin equivalent that models the grid. In actuality, DC VSC terminals may be linked to a variety of renewable energy sources. The three distinct DC sources evaluated in this study are shown in Fig. 2. In Fig. 2a, the left panel shows a battery. A variable speed type-IV (full converter) wind generator with a wind turbine connected to an electric generator managed by a back-end converter is shown in the middle panel (Fig. 2b). The last panel (Fig. 2c) on the right shows a photovoltaic (PV) generator. Ibat represents the battery's produced current, Ifc represents the DC current from the whole converter, and Ipv represents the current from the photovoltaic generator.

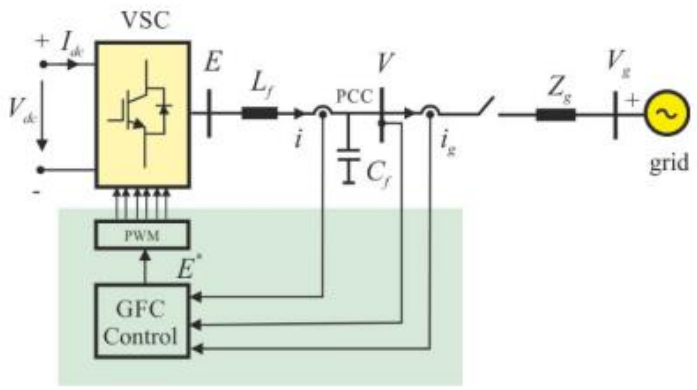


FIGURE 5.1. System description of a three-phase grid-forming voltage source converter connected to the grid.

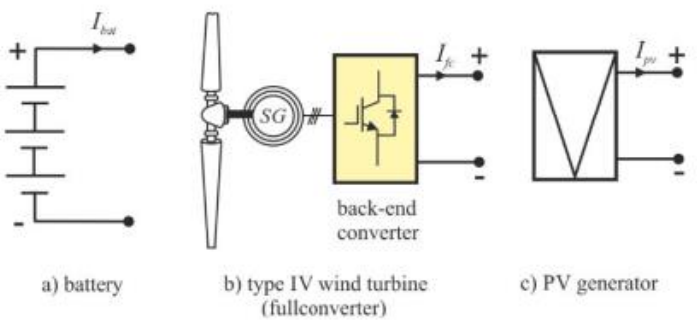


FIGURE 5.2. DC sources: a) battery, b) wind turbine, c) PV generator.

**REACTIVE POWER SYNCHRONIZATION**

The model shown in Fig. 3 is used to evaluate the current relationship between the instantaneous active and reactive powers produced by the GFC against an increase in voltage and angle. The grid with frequency ω0 is represented by the GFC in this diagram as a voltage source behind an impedance. Grid impedance is given as Zg = Rg + jω0Lg, and the grid voltage is assumed to be a phase reference of Vg = Vg 6 0. The angular difference between the two voltages is represented by the angle, δ, and the GFC voltage is V = V6 δ.

International Journal of Engineering Research and Science & Technology

ISSN 2319-5991 www.ijerst.com

Vol. 17, Issue.2, 2024

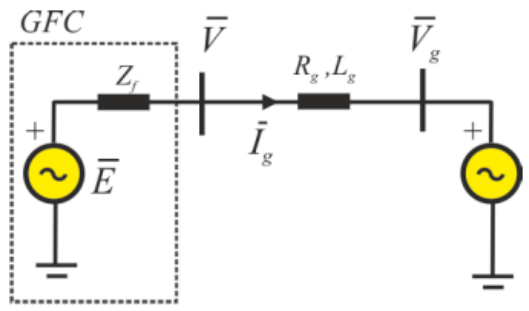


FIGURE 5.3. Simplified representation of a GFC connected to a grid.

Complex power, Sg = Pg + jQg, is calculated in steady state based on PCC output as

$$\bar{S}_g = P_g + jQ_g = \bar{V}\left(\frac{\bar{V} - \bar{V}_g}{\bar{Z}_g}\right)^* \qquad (1)$$

where each magnitude is represented as a unit (pu). The current phasor, I g, is indicated by the word in parenthesis, and the corresponding complex conjugate is denoted by the symbol (∗). The voltage and current phasor vector diagram is shown in Fig. 4.

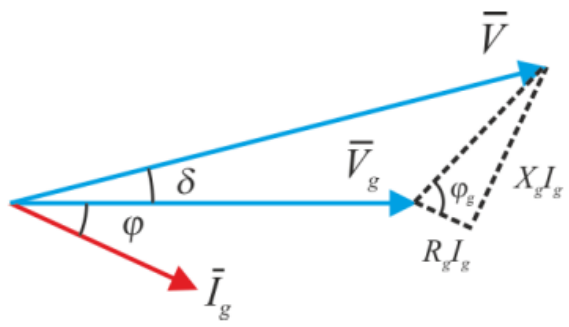


FIGURE 4. Voltages and current vector diagram.

Considering Zg = Zge jϕg and separating the real and imaginary parts, the active and reactive powers can be expressed as follows:

$$P_g = \frac{V}{Z_g}\left(V\cos\varphi_g - V_g\cos(\varphi_g + \delta)\right)$$
$$Q_g = \frac{V}{Z_g}\left(V\sin\varphi_g - V_g\sin(\varphi_g + \delta)\right). \qquad (2)$$

If $R_g = 0$, then

$$P_g = \frac{VV_g}{X_g}\sin\delta \quad Q_g = \left(\frac{V}{X_g}\right)\left(V - V_g\cos\delta\right). \qquad (3)$$

The dynamic equations for the circuit illustrated in Fig. 3 expressed in per unit for a dq reference frame rotating at a speed of ω0 a

$$\bar{V} - \bar{V}_g = R_g\bar{I}_g + \frac{L_g}{\omega_0}\frac{d\bar{I}_g}{dt} + jL_g\bar{I}_g \qquad (4)$$

where V = vd + jvq, Vg = vdg + jvqg, and I g = idg + jiqg. When considering voltage, Vg, as a reference, the vqg component is zero, and the voltages vd = Vcosδ and vq = Vsinδ. Taking the real and imaginary parts in (4), we obtain the following dynamic equation

$$V\cos\delta - V_g = R_g i_{dg} + \frac{L_g}{\omega_0}\frac{di_{dg}}{dt} - L_g i_{qg}$$
$$V\sin\delta = R_g i_{qg} + \frac{L_g}{\omega_0}\frac{di_{qg}}{dt} + L_g i_{dg}. \qquad (5)$$

The state variables of this system are idg and iqg, and the inputs are V, Vg, and δ, where the values of the active and reactive powers a

$$P_g = v_d i_{dg} + v_q i_{qg} = (V\cos\delta)\, i_{dg} + (V\sin\delta)\, i_{qg}$$
$$Q_g = v_q i_{dg} - v_d i_{qg} = (V\sin\delta)\, i_{dg} - (V\cos\delta)\, i_{qg}. \qquad (6)$$

Next, the variations of the instantaneous active and reactive powers transmitted by the GFC after an angle step of δ and a voltage step of V are obtained. The grid parameter values are as follows: Rg = 0.01 pu and Lg = 0.15 pu (Zg = 0.1503 pu and ϕg = 86.19◦ ) at a frequency of 50 Hz (ω0 = 100π rad/s

### A. VOLTAGE ANGLE STEP

Fig. 5.4 denotes the transient variation of Pg and Qg at t = 0.1 s, when a step of δ = 8.62◦ is generated against the grid voltage. Here, the GFC and grid voltage magnitude both remain constant at V = Vg = 1

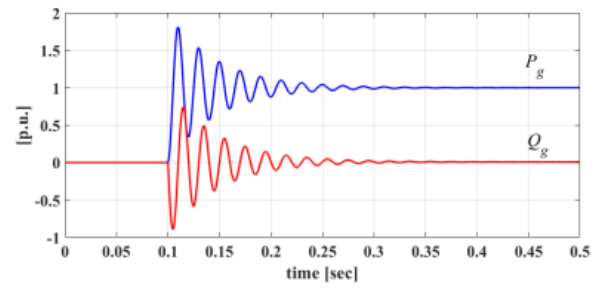


FIGURE 5.4 . Active and reactive power response to a step in the GFC voltage angl

As can observed, the active power increases until matching its steady-state value of Pg = 1 pu through damped oscillation. Reactive power also oscillates until it reaches its steadystate value of Qg = 0.09 pu. Both powers converge to their steady-state values, but during their transient state, power oscillations are similar in amplitude although they pulse in counter phase. Fig. 6 displays the power values recorded in a PQ plot. This figure clearly denotes the damped oscillation of both powers describing a spiral starting from the (0,0) point and converging on the final steady-state point at (1, 0.089). The spiral is traversed from left to right in such a way that, as the active power increases, the reactive power decreas

### B. VOLTAGE AMPLITUDE STEP

The same analysis is conducted when the magnitude of the GFC voltage changes from V = 1 to 1.075 pu. The voltage angle at the PCC is held constant and equal to δ = 0 ◦ . Fig. 7 denotes the transient variation of the act

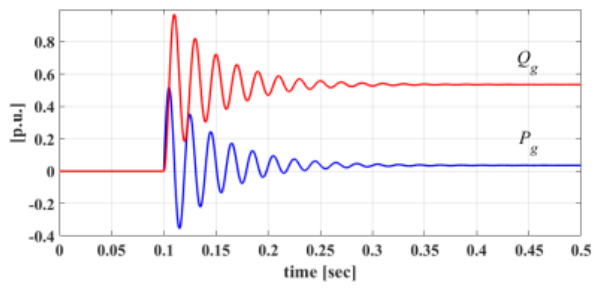


FIGURE 5.5 . Active and reactive power response to a step in the GFC voltage amplitude.

as well as responsive abilities. While both powers fluctuate in phases, the reactive power rises until it achieves its steady-state value at Qg = 0.5 pu, while the active power stays almost constant. Furthermore, a spiral from the (0,0) point to (0.02,0.5) pu is described by the powers on the PQ plane. Here, the two powers fluctuate in phases; that is, a rise in the active power results in a corresponding rise in the reactive power, and vice versa. The development of the Pg and Qg powers in the PQ plane against variations in the amplitude of the PCC voltage is seen in Fig. 8.

### 5.1 GRID-FORMING CONVERTER CONTROL

The RPS block in Figure 9 represents the overall architecture of the reactive power synchronization-based GFC control system. Measurements are made of the current at the converter's output, [i]abc, and the instantaneous currents of the three-phase grid, represented by the [i]g,abc, in order to carry out this control. The instantaneous PCC voltages are also expressed as [v]abc.

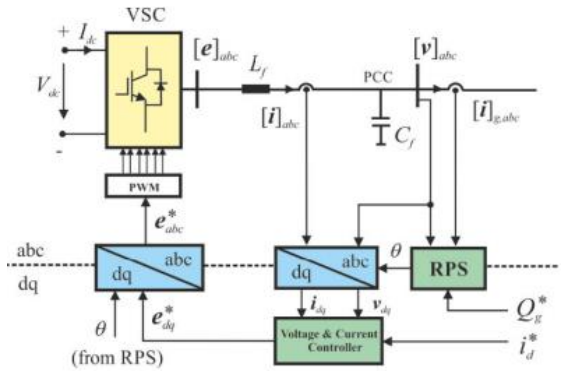


FIGURE 5.5. General scheme of the GFC control.

This control obtains the angle, θ , through the RPS block, which positions the d axis in a dq rotary axes system with respect to a stationary reference axis, α (Fig. 10). The angle, θ , is then used to determine the dq components of the current at the output of the converter idq = id + jiq, as well as the PPC dq voltages vdq = vd +jvq, through a Park transformation (abc/dq). The voltage and current controllers use these variables as input to align the PCC

International Journal of Engineering Research and Science & Technology

ISSN 2319-5991 www.ijerst.com

Vol. 17, Issue.2, 2024

voltage vector toward the d axis of the rotary system (vq = 0) and to control the reference current, i ∗ d , which is associated with the active power generated when the vdq voltage vector is oriented toward the d axis.

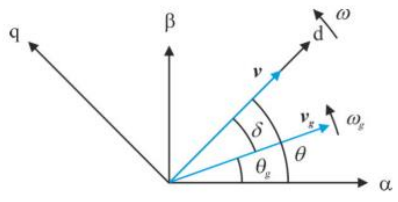


FIGURE 10. Voltage vector diagram.

The PCC, v, and grid, vg, voltage vector diagrams are shown in Fig. 10. The v voltage vector, as previously stated, rotates at a speed of ω and maintains its regulated alignment with the d axis. Its angular location with respect to the reference axis is □. The vg vector spins at a speed of ωg, resulting in the formation of an angle of θg. The angular difference between the two vectors is represented by the angle, δ, which stays constant when ω = ωg. In a stable condition, the active power delivered from the grid to the GFC is proportional to sinδ, as per equation (3). The formula that follows determines the dynamics of the power angle, δ:

where the control system and grid frequencies, given in pu, are represented by ω and ωg, respectively.

### A. SYNCHRONIZATION BLOCK WITH REACTIVE POWER

The reactive power, Qg, and power angle, δ, have a dynamic connection when the GFC delivers the active power, Pg, to the grid, as was covered in Section III. This connection will serve as a means of synchronization. The RPS block's reactive power synchronization loop is shown in Fig. 11. To get an angle of θ via the synchronization constant, Ks, the per unit frequency increase, 1ω, that must be applied to the control is determined by the difference between the reference reactive power, Q ∗ g, and the reactive power measured at the GFC output, Qg.

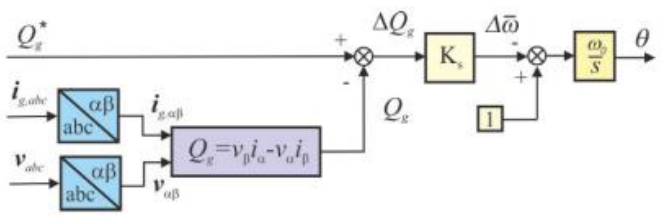


FIGURE 11. Reactive power synchronization loop.

Reactive power is calculated using the GFC's output, which is represented in normalized values for the instantaneous values of [i]g,abc and [v]abc by the use of a Clarke transformation. The produced reactive power, Q ∗ g = Qg, equals the reference power when the grid is synchronized at a frequency of ω0, or 1ω = 0. In the event that the grid frequency deviates from ω0, the synchronization loop will use Q ∗ g 6= Qg to offset the frequency divergence. The GFC enters an islanded state and the currents of the [i]g,abc vector become nil if the main breaker trips. A load connected to the GFC terminals would have a feeding frequency of ω0 under this situation of 1Qg = 0. In this case, the RPS block does not follow the current PCC voltage angle as a PLL would. Rather, after sensing the reactive power, it modifies the internal frequency increase, 1ω, to produce a synchronization component. The GFC may function in islanded mode by adjusting the PCC voltage amplitude and frequency settings after the main breaker trips, as will be covered in the sections that follow. That won't occur, however, if the converter is in grid-following mode. Without an appropriate control reference, the PLL monitors the produced voltage angle when the breaker trips.

### B. CURRENT AND VOLTAGE CONTROLLER

The GFC controller, as shown in Fig. 9, uses the angle, θ, found in the RPS block to perform the Park transformation before receiving the dq values from the [i]abc currents and [v]abc voltages. This controller maintains the voltage vector aligned to the d axis from the reference rotational system, meaning that vq = 0, by having an outer voltage control loop and an inner current control loop for the dq components. A block schematic for the dq current and voltage controller is shown in Fig. 12.

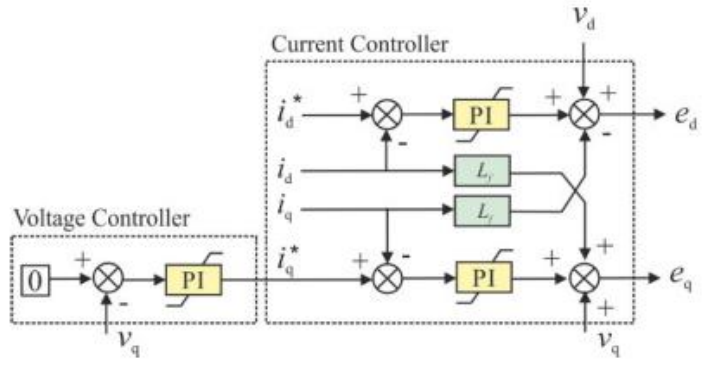


FIGURE 12. Outer voltage controller and Inner current controller.

The outer voltage controller maintains the voltage vector oriented by establishing that v ∗ q = 0 by regulating the current, iq. This is possible because the dynamic equations in the filter capacitor, Cf , describe the relationship between current and voltage in each of the dq axes. These equations, expressed in normalized values, are

$$i_d - i_{dg} = \frac{C_f}{\omega_0}\frac{dv_d}{dt} - C_f v_q$$
$$i_q - i_{qg} = \frac{C_f}{\omega_0}\frac{dv_q}{dt} + C_f v_d. \qquad (22)$$

The second equation in (22) shows how the fluctuation of vq is controlled by the current, iq; the disturbance variables of the voltage control loop are represented by the terms iqg and Cf vd. In the first equation, in a steady state, the current, id, equals idg when the voltage is directed toward the rotating reference system (vq = 0). As a result, the power sent to the grid and the GFC active power are equal. In a transient condition, the voltage, vd, which is equal to the magnitude of the PCC voltage, is altered by the difference between the two currents. This demonstrates that, while running in islanding mode, the PCC voltage magnitude may be changed by active power by varying the current reference i ∗ d. In the event that the GFC runs in an islanded mode, the power required by the load is obtained by voltage management via active power. However, as the power setpoint is only used to draw a certain quantity of power from the source, the active power cannot be used to control PCC voltage while the GFC is connected to the grid. Consequently, in grid-connected mode, the Q ∗ g value is often modified to exchange reactive power and manage the voltage (Fig. 9). According to the filter capacitor equations, this logic holds true even if the GFC's output filter is type L [22], [25], and [26].

## 6. MATLAB MODELING AND SIMULATION

### 6.1 SIMULATION CIRCUITS

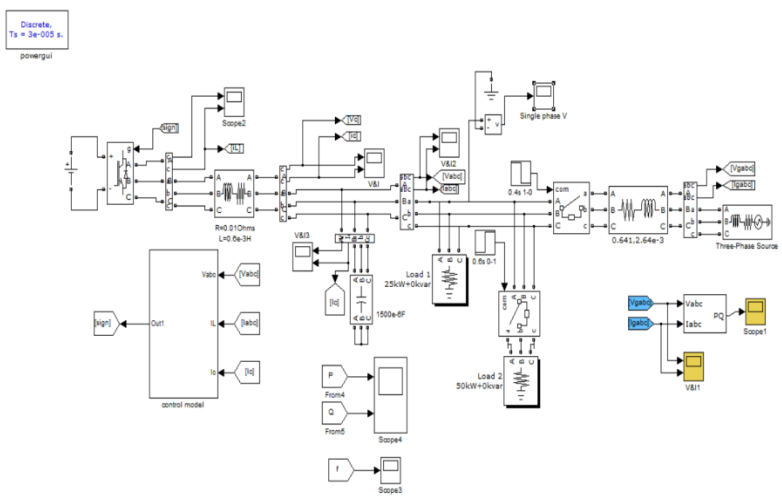


Fig6.1 simulation Circuit

International Journal of Engineering Research and Science & Technology

ISSN 2319-5991 www.ijerst.com

Vol. 17, Issue.2, 2024

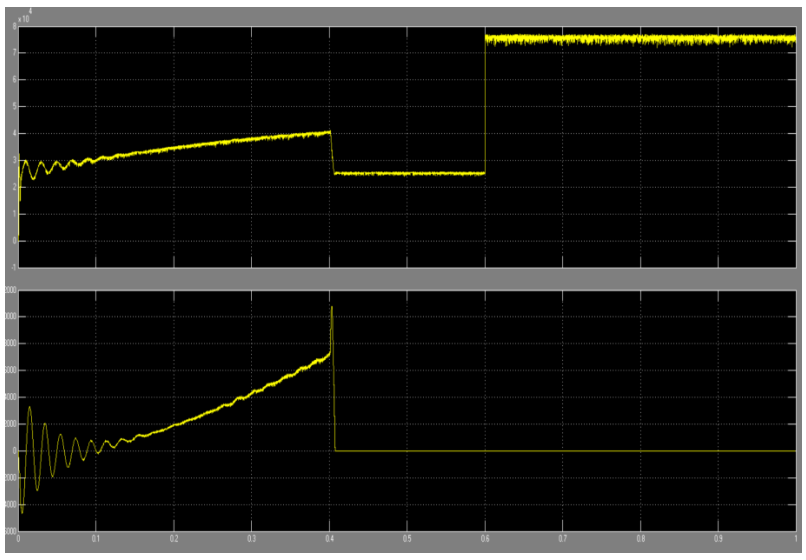

Fig 6.2 Active ad reactive power

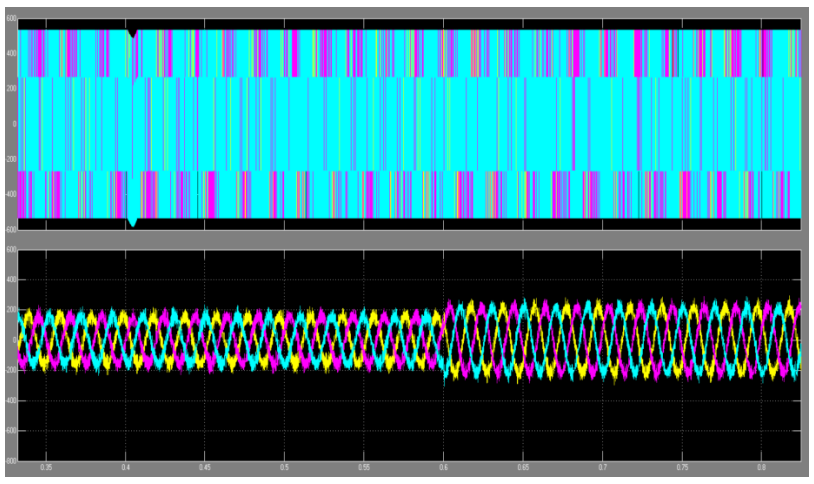

Fig 6.3 Source voltage ad current

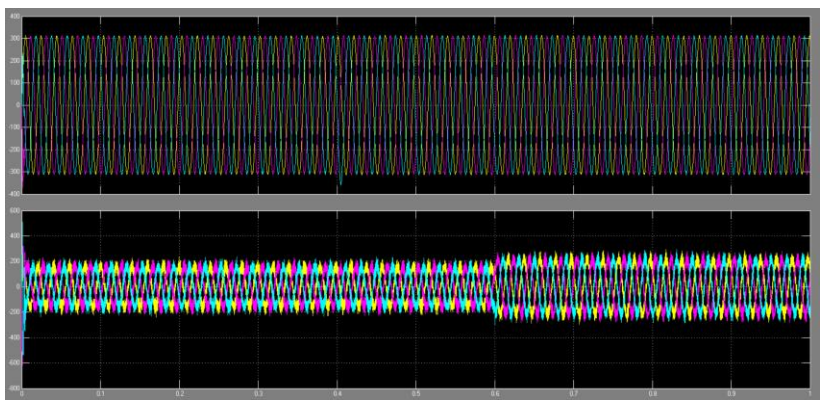

Fig 6.4. Load voltage ad current

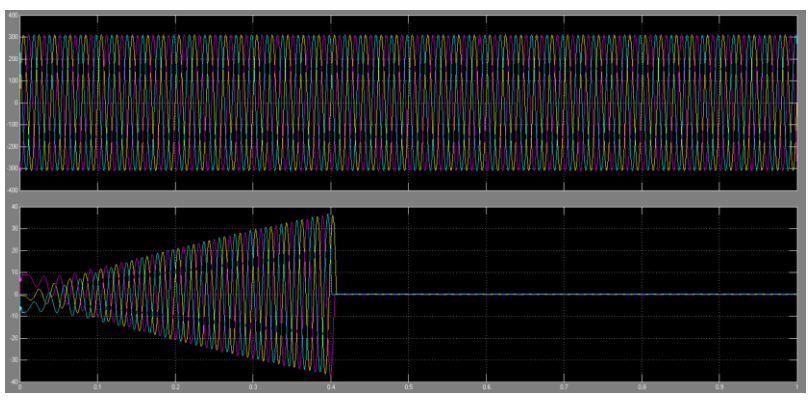

Fig 6.5. grid voltage ad current

## CONCLUSION

This paper suggests a new GFC control system for renewable energy facilities, including as PV plants, FC wind turbines, and batteries, that is based on the RPS technique. This study first presents an overview of the RPS approach, describing the transfer function between 1Qg and 1δ and the dynamic coupling between the instantaneous active and reactive powers, which enables the synchronization process to be carried out. The primary benefit of this system over previous APS techniques is that it permits the separation of the active power control and synchronization loops, hence enabling the effective integration of the various generating sources linked to the DC input bus.

TABLE 1. Li-ion battery parameters.

| PARAMETER | SYMBOL | VALUE | UNITS |
|---|---|---|---|
| Maximum voltage | $V_{max}$ | 900 | V |
| Nominal voltage | $V_n$ | 800 | V |
| Minimum voltage | $V_{min}$ | 600 | V |
| Exponential voltage | $V_{exp}$ | 825 | V |
| Nominal capacity | $Q_n$ | 1300 | Ah |
| Exponential capacity | $Q_{exp}$ | 100 | Ah |
| Battery constant voltage | $E_0$ | 858 | V |
| Polarization voltage | $K$ | 38.5 | Ah |
| Exponential zone amplitude | $A$ | 81 | V |
| Exponential zone time constant inverse | $B$ | 0.03 | $Ah^{-1}$ |
| Internal resistance | $R_s$ | 16 | $m\Omega$ |
| Capacitance | $C_b$ | 85 | $F$ |
| Parallel resistance | $R_p$ | 22.5 | $m\Omega$ |

This research also presents several models and control techniques for batteries connected to a GFC converter, FC wind turbines, and PV plants. Subsequently, the research suggests a GFC–RPS control system and confirms its efficacy in various scenarios. When a load variation event occurs on the grid, P/F regulation is the initial application. Batteries and FC wind turbines via FFR from the internal control variable, 1ω, are used to offer this service. This service is only available for PV plants if the initial power output is less than the maximum power point. In conclusion, PV plants are capable of providing this service, but at the great economic cost of a large energy output loss. This paper then demonstrates the GFC–RPS control's ability to exchange reactive power with the grid in a grid-following mode in response to voltage variations at its terminals. It also shows how the suggested system can regulate the output terminals' AC voltage by exchanging reactive power, even when this variable is connected to the synchronization loop. Ultimately, the GFC's exceptional dynamic responsiveness is confirmed via the process of switching from a grid-connected to an islanded mode while providing a dynamic load. The findings showed that the voltage and frequency stay constant throughout the transition, proving that the suggested GFC control does, in fact, function as a real voltage source that mimics the characteristics of a traditional SG.

## REFERENCES

[1] Received April 13, 2021, accepted April 29, 2021, date of publication May 6, 2021, date of current version May 13, 2021.Digital Object Identifier 10.1109/ACCESS.2021.3078078 Grid-Forming Converters Control Based on the Reactive Power Synchronization Method for Renewable Power Plants.

[2] R. H. Lasseter, ‘‘Microgrids,’’ in Proc. IEEE Power Eng. Soc. Winter Meeting Conf., vol. 1, Jan. 2002, pp. 305–308.

[3] J. Rocabert, A. Luna, F. Blaabjerg, and P. Rodriguez, ‘‘Control of power converters in AC microgrids,’’ IEEE Trans. Power Electron., vol. 27, no. 11, pp. 4734–4749, Nov. 2012.

[4] P. Christensen, G. K. Andersen, M. Seidel, S. Bolik, S. Engelken, T. Knueppel, A. Krontiris, K. Wuerflinger, T. Bülo, J. Jahn, and M. Ndreko, ‘‘High penetration of power electronic interfaced power sources and the potential contribution of grid forming converters,’’ ENTSO-E, Brussels, Belgium, Tech. Rep. 1, 2020.

[5] Establishing a Network Code on Requirements for Grid Connection of Generators, Commission Regulation (EU) 2016/631, Brussels, Belgium, 2016.

ISSN 2319-5991 www.ijerst.com
Vol. 17, Issue.2, 2024

[6] N. Hatziargyriou, ‘‘Task force on definition and characterization of dynamic behavior in systems with high penetration of power electronic interfaced technologies,’’ Power Energy Soc., Piscataway, NJ, USA, Tech. Rep. PES-TR77, 2020.

[7] B. Yu, M. Matsui, and G. Yu, ‘‘A review of current anti-islanding methods for photovoltaic power system,’’ Sol. Energy, vol. 84, no. 5, pp. 745–754, May 2010.

[8] R. Teodorescu, M. Liserre, and P. Rodriguez, Grid Converters for Photovoltaic and Wind Power Systems, vol. 29. Hoboken, NJ, USA: Wiley, 2011.

[9] A. Luna, J. Rocabert, J. I. Candela, J. R. Hermoso, R. Teodorescu, F. Blaabjerg, and P. Rodriguez, ‘‘Grid voltage synchronization for distributed generation systems under grid fault conditions,’’ IEEE Trans. Ind. Appl., vol. 51, no. 4, pp. 3414–3425, Jul. 2015.

[10] M. Karimi-Ghartemani, ‘‘A unifying approach to single-phase synchronous reference frame PLLs,’’ IEEE Trans. Power Electron., vol. 28, no. 10, pp. 4550–4556, Oct. 2013.

[11] X. Wang and F. Blaabjerg, ‘‘Harmonic stability in power electronic-based power systems: Concept, modeling, and analysis,’’ IEEE Trans. Smart Grid, vol. 10, no. 3, pp. 2858–2870, May 2019.